Dijet azimuthal decorrelations at the LHC in the Regge limit of QCD

M.A. Nefedov, V.A. Saleev, A.V. Shipilova

Samara State University

03.06.2014, Quarks-2014, Suzdal, Russia

Outline

Introduction

Parton Reggeization Approach

Dijet production

$b\bar{b}$-pair production

Prompt-photon plus jet production

Summary and Conclusions

Production of two high-p_T jets

Motivation

- Multiple jet production is the dominant high transverse-momentum (p_T) process at LHC energies.
- Azimuthal decorrelations between the two central jets with the largest transverse momenta are sensitive to the dynamics of events with multiple jets.
- Particularly, the measurements of decorrelations in the azimuthal angle between the two most energetic jets, $\Delta\varphi$, as a function of number of produced jets, give the chance to separate directly leading order (LO) and next-to-leading orders (NLO) contributions in the strong coupling constant α_S.
- A detailed understanding of events with large azimuthal decorrelations is important to searches for new physical phenomena with dijet signatures, such as supersymmetric extensions to the Standard Model.

Production of two high-p_T jets

Motivation

- Multiple jet production is the dominant high transverse-momentum (p_T) process at LHC energies.
- Azimuthal decorrelations between the two central jets with the largest transverse momenta are sensitive to the dynamics of events with multiple jets.
- Particularly, the measurements of decorrelations in the azimuthal angle between the two most energetic jets, $\Delta\varphi$, as a function of number of produced jets, give the chance to separate directly leading order (LO) and next-to-leading orders (NLO) contributions in the strong coupling constant α_S.
- A detailed understanding of events with large azimuthal decorrelations is important to searches for new physical phenomena with dijet signatures, such as supersymmetric extensions to the Standard Model.

Production of two high-p_T jets

Motivation

- Multiple jet production is the dominant high transverse-momentum (p_T) process at LHC energies.
- Azimuthal decorrelations between the two central jets with the largest transverse momenta are sensitive to the dynamics of events with multiple jets.
- Particularly, the measurements of decorrelations in the azimuthal angle between the two most energetic jets, $\Delta\varphi$, as a function of number of produced jets, give the chance to separate directly leading order (LO) and next-to-leading orders (NLO) contributions in the strong coupling constant α_S.
- A detailed understanding of events with large azimuthal decorrelations is important to searches for new physical phenomena with dijet signatures, such as supersymmetric extensions to the Standard Model.

Production of two high-p_T jets

Motivation

- Multiple jet production is the dominant high transverse-momentum (p_T) process at LHC energies.
- Azimuthal decorrelations between the two central jets with the largest transverse momenta are sensitive to the dynamics of events with multiple jets.
- Particularly, the measurements of decorrelations in the azimuthal angle between the two most energetic jets, $\Delta\varphi$, as a function of number of produced jets, give the chance to separate directly leading order (LO) and next-to-leading orders (NLO) contributions in the strong coupling constant α_S.
- A detailed understanding of events with large azimuthal decorrelations is important to searches for new physical phenomena with dijet signatures, such as supersymmetric extensions to the Standard Model.

Production of two high-p_T jets

Experimental studies

- ATLAS Collaboration: $\sqrt{S} = 7$ TeV,$p_T > 30$ GeV, $|y_{jj}| < 1.1$
  G. Aad et al., Measurement of Dijet Azimuthal Decorrelations in pp Collisions at $\sqrt{S} = 7$ TeV, Phys. Rev. Lett. **106***, 172002 (2011).*
- CMS Collaboration: $\sqrt{S} = 7$ TeV,$p_T > 100$ GeV, $|y_{jj}| < 0.8$
  V. Khachatryan at al., Dijet Azimuthal Decorrelations in pp Collisions at $\sqrt{S} = 7$ TeV, Phys. Rev. Lett. **106***, 122003 (2011).*

Theoretical studies

- pQCD calculations, next-to-leading order (NLO) in three-parton production: Z. Nagy, Phys. Rev. D 68, 094002 (2003), Phys. Rev. Lett. 88, 122003 (2002).
- Event generators: PYTHIA, HERWIG, SHERPA, MADGRAPH, ...

Production of two high-p_T jets

Experimental studies

- ATLAS Collaboration: $\sqrt{S} = 7$ TeV,$p_T > 30$ GeV, $|y_{jj}| < 1.1$
  G. Aad et al., Measurement of Dijet Azimuthal Decorrelations in pp Collisions at $\sqrt{S} = 7$ TeV, Phys. Rev. Lett. **106***, 172002 (2011).*
- CMS Collaboration: $\sqrt{S} = 7$ TeV,$p_T > 100$ GeV, $|y_{jj}| < 0.8$
  V. Khachatryan at al., Dijet Azimuthal Decorrelations in pp Collisions at $\sqrt{S} = 7$ TeV, Phys. Rev. Lett. **106***, 122003 (2011).*

Theoretical studies

- pQCD calculations, next-to-leading order (NLO) in three-parton production: Z. Nagy, Phys. Rev. D 68, 094002 (2003), Phys. Rev. Lett. 88, 122003 (2002).
- Event generators: PYTHIA, HERWIG, SHERPA, MADGRAPH, ...

Production of two high-p_T jets

Experimental studies

- ATLAS Collaboration: $\sqrt{S} = 7$ TeV,$p_T > 30$ GeV, $|y_{jj}| < 1.1$
  G. Aad et al., Measurement of Dijet Azimuthal Decorrelations in pp Collisions at $\sqrt{S} = 7$ TeV, Phys. Rev. Lett. **106**, *172002 (2011).*
- CMS Collaboration: $\sqrt{S} = 7$ TeV,$p_T > 100$ GeV, $|y_{jj}| < 0.8$
  V. Khachatryan at al., Dijet Azimuthal Decorrelations in pp Collisions at $\sqrt{S} = 7$ TeV, Phys. Rev. Lett. **106**, *122003 (2011).*

Theoretical studies

- pQCD calculations, next-to-leading order (NLO) in three-parton production: Z. Nagy, Phys. Rev. D 68, 094002 (2003), Phys. Rev. Lett. 88, 122003 (2002).
- Event generators: PYTHIA, HERWIG, SHERPA, MADGRAPH, ...

Production of two high-p_T jets

Experimental studies

- ATLAS Collaboration: $\sqrt{S} = 7$ TeV,$p_T > 30$ GeV, $|y_{jj}| < 1.1$
  G. Aad et al., Measurement of Dijet Azimuthal Decorrelations in pp Collisions at $\sqrt{S} = 7$ TeV, Phys. Rev. Lett. **106**, *172002 (2011).*
- CMS Collaboration: $\sqrt{S} = 7$ TeV,$p_T > 100$ GeV, $|y_{jj}| < 0.8$
  V. Khachatryan at al., Dijet Azimuthal Decorrelations in pp Collisions at $\sqrt{S} = 7$ TeV, Phys. Rev. Lett. **106**, *122003 (2011).*

Theoretical studies

- pQCD calculations, next-to-leading order (NLO) in three-parton production: Z. Nagy, Phys. Rev. D 68, 094002 (2003), Phys. Rev. Lett. 88, 122003 (2002).
- Event generators: PYTHIA, HERWIG, SHERPA, MADGRAPH, ...

Particle production at large $\sqrt{S}$

Higher-order perturbative corrections:

- Heavy final states (Higgs bosons, $t\bar{t}$, ...) produced by large-$x \sim 10^{-1}$ initial partons $\leftarrow$ soft and collinear gluons
- Light final states (small-p_T quarkonia, single jets, prompt photons, ...) produced by small-$x \sim 10^{-3}$ $\leftarrow$ additional hard jets $\leftarrow$ higher-order corrections in α_s $\Rightarrow$ complicated task

k_T-factorization approach: works with off-shell initial-state partons with a significant transverse momentum $|\mathbf{q}_T| \sim x\sqrt{S}$. The factorization formula:

$$d\sigma(\mathcal{Y}) = \sum_{i,j} \Phi_i(x_1, |\mathbf{q}_{1T}|^2, \mu_F) \otimes \Phi_j(x_2, |\mathbf{q}_{2T}|^2, \mu_F) \otimes \otimes d\hat{\sigma}_{ij}(x_1, |\mathbf{q}_{1T}|; x_2, |\mathbf{q}_{2T}|, \mathcal{Y}),$$

$\Phi_i(x_i, |\mathbf{q}_{iT}|^2, \mu_F)$ – unintegrated parton distribution function

μ_F separates stages of the unPDF evolution and the hard scattering

Particle production at large $\sqrt{S}$

Higher-order perturbative corrections:

- Heavy final states (Higgs bosons, $t\bar{t}$, ...) produced by large-$x \sim 10^{-1}$ initial partons $\leftarrow$ soft and collinear gluons
- Light final states (small-p_T quarkonia, single jets, prompt photons, ...) produced by small-$x \sim 10^{-3} \leftarrow$ additional hard jets $\leftarrow$ higher-order corrections in $\alpha_s \Rightarrow$ complicated task

k_T-factorization approach: works with off-shell initial-state partons with a significant transverse momentum $|\mathbf{q_T}| \sim x\sqrt{S}$. The factorization formula:

$$\begin{aligned} d\sigma(\mathcal{Y}) &= \sum_{i,j} \Phi_i(x_1, |\mathbf{q}_{1T}|^2, \mu_F) \otimes \Phi_j(x_2, |\mathbf{q}_{2T}|^2, \mu_F) \otimes \\ &\otimes \quad d\hat{\sigma}_{ij}(x_1, |\mathbf{q}_{1T}|; x_2, |\mathbf{q}_{2T}|, \mathcal{Y}), \end{aligned}$$

$\Phi_i(x_i, |\mathbf{q}_{iT}|^2, \mu_F)$ – unintegrated parton distribution function

μ_F separates stages of the unPDF evolution and the hard scattering

Unintegrated PDFs

Normalization condition:

$$xF_g^{p,\bar{p}}(x,\mu^2) = \int^{\mu^2} \Phi_g^{p,\bar{p}}(x,|\mathbf{q_T}|^2,\mu^2)d|\mathbf{q_T}|^2$$

In the asymptotic high-energy limit of QCD (Regge regime): $\Lambda_{QCD} \ll \mu_F \sim \mu_R \ll \sqrt{S} \to$ the dominant large logarithms of type $\log(1/x) \Rightarrow$ BFKL evolution equation
We use the KMR PDF (M. A. Kimber, A. D. Martin, M. G. Ryskin, G. Watt, 2001–2004) with input set of integrated ones of A. D. Martin, R. G. Roberts , V. G. Stirling , R. S. Thorne, 2002 (MRST2002).

KMR PDFs are based on Dokshitzer-Gribov-Lipatov-Altarelli-Parisi (DGLAP) evolution equations with contribution of the large logarithms $\log(\frac{\mu^2}{\Lambda^2_{QCD}})$ and include additionally (model dependent) BFKL corrections due to large logarithms $\log(\frac{S}{\mu^2}) \simeq \log(\frac{1}{x})$. The KMR procedure (realized as the open code in C++) is constructed in the way which takes into account the gluon Reggeization and so far it is clear to use it together with Reggeon effective vertices.

Unintegrated PDFs

Normalization condition:

$$xF_g^{p,\bar{p}}(x,\mu^2) = \int^{\mu^2} \Phi_g^{p,\bar{p}}(x,|\mathbf{q_T}|^2,\mu^2)d|\mathbf{q_T}|^2$$

In the asymptotic high-energy limit of QCD (Regge regime): $\Lambda_{QCD} \ll \mu_F \sim \mu_R \ll \sqrt{S} \to$ the dominant large logarithms of type $\log(1/x) \Rightarrow$ BFKL evolution equation

We use the KMR PDF (M. A. Kimber, A. D. Martin, M. G. Ryskin, G. Watt, 2001–2004) with input set of integrated ones of A. D. Martin, R. G. Roberts , V. G. Stirling , R. S. Thorne, 2002 (MRST2002).

KMR PDFs are based on Dokshitzer-Gribov-Lipatov-Altarelli-Parisi (DGLAP) evolution equations with contribution of the large logarithms $\log(\frac{\mu^2}{\Lambda^2_{QCD}})$ and include additionally (model dependent) BFKL corrections due to large logarithms $\log(\frac{S}{\mu^2}) \simeq \log(\frac{1}{x})$. The KMR procedure (realized as the open code in C++) is constructed in the way which takes into account the gluon Reggeization and so far it is clear to use it together with Reggeon effective vertices.

Unintegrated PDFs

Normalization condition:

$$xF_g^{p,\bar{p}}(x,\mu^2) = \int^{\mu^2} \Phi_g^{p,\bar{p}}(x,|\mathbf{q_T}|^2,\mu^2)d|\mathbf{q_T}|^2$$

In the asymptotic high-energy limit of QCD (Regge regime):
$\Lambda_{QCD} \ll \mu_F \sim \mu_R \ll \sqrt{S} \rightarrow$ the dominant large logarithms of type $\log(1/x) \Rightarrow$ BFKL evolution equation
We use the KMR PDF (M. A. Kimber, A. D. Martin, M. G. Ryskin, G. Watt, 2001–2004) with input set of integrated ones of A. D. Martin, R. G. Roberts , V. G. Stirling , R. S. Thorne, 2002 (MRST2002).

KMR PDFs are based on Dokshitzer-Gribov-Lipatov-Altarelli-Parisi (DGLAP) evolution equations with contribution of the large logarithms $\log(\frac{\mu^2}{\Lambda^2_{QCD}})$ and include additionally (model dependent) BFKL corrections due to large logarithms $\log(\frac{S}{\mu^2}) \simeq \log(\frac{1}{x})$. The KMR procedure (realized as the open code in C++) is constructed in the way which takes into account the gluon Reggeization and so far it is clear to use it together with Reggeon effective vertices.

Unintegrated PDFs

Normalization condition:

$$xF_g^{p,\bar{p}}(x,\mu^2) = \int^{\mu^2} \Phi_g^{p,\bar{p}}(x,|\mathbf{q_T}|^2,\mu^2)d|\mathbf{q_T}|^2$$

In the asymptotic high-energy limit of QCD (Regge regime): $\Lambda_{QCD} \ll \mu_F \sim \mu_R \ll \sqrt{S} \to$ the dominant large logarithms of type $\log(1/x) \Rightarrow$ BFKL evolution equation
We use the KMR PDF (M. A. Kimber, A. D. Martin, M. G. Ryskin, G. Watt, 2001–2004) with input set of integrated ones of A. D. Martin, R. G. Roberts , V. G. Stirling , R. S. Thorne, 2002 (MRST2002).

KMR PDFs are based on Dokshitzer-Gribov-Lipatov-Altarelli-Parisi (DGLAP) evolution equations with contribution of the large logarithms $\log(\frac{\mu^2}{\Lambda^2_{QCD}})$ and include additionally (model dependent) BFKL corrections due to large logarithms $\log(\frac{S}{\mu^2}) \simeq \log(\frac{1}{x})$. The KMR procedure (realized as the open code in C++) is constructed in the way which takes into account the gluon Reggeization and so far it is clear to use it together with Reggeon effective vertices.

Unintegrated gluon distribution functions: KMR prescription.

- The formalism embodies both DGLAP and BFKL contributions.
- The key observation is that the μ dependence of the unintegrated distributions enters at the last step of the evolution, so single-scale evolution equations can be used.
- The parton distributions $\Phi_a^h(x, q_T^2, \mu^2)$, $a = q, g$, unintegrated over the transverse momentum q_T, are calculated from auxiliary functions $h_a(x, q_T^2)$, which satisfy single-scale evolution equations.
- An advantage of the single-scale unified BFKL/DGLAP equation is that it incorporates a major part of the subleading order $\ln(1/x)$ (BFKL) effects.

$$\Phi_g(x, q_T^2, \mu^2) = T_g(q_T, \mu) \frac{\alpha_s(q_T^2)}{2\pi} \times$$

$$\times \quad \left(\int_x^{\mu/(\mu+q_T)} dz \int^{q_T^2} \frac{dk_T^2}{k_T^2} \left[\bar{P}(z) h_g(x/z, k_T^2) + P_{gq}(z) \sum h_q(x/z, k_T^2) \right] + \right.$$

$$\left. + \quad 2N_c \int_x^{\mu/(\mu+k_T)} \frac{dz}{z} \int \frac{d^2p}{\pi p^2} \left[\frac{q_T^2}{k_T^2} h_g(x/z, k_T^2) - \theta(q_T^2 - p^2) h_g(x/z, q_T^2) \right] \right),$$

$$T_g(q_T, \mu) = \exp\left(- \int_{q_T^2}^{\mu^2} \frac{\alpha_s(k_T^2)}{2\pi} \frac{dk_T^2}{k_T^2} \sum_a \int_0^{1-\Delta} P_{ag}(z) dz \right),$$

$$\bar{P}(z) = P_{gg}(z) - 2N_c/z.$$

Unintegrated gluon distribution functions: KMR prescription.

- The formalism embodies both DGLAP and BFKL contributions.
- The key observation is that the μ dependence of the unintegrated distributions enters at the last step of the evolution, so single-scale evolution equations can be used.
- The parton distributions $\Phi_a^h(x, q_T^2, \mu^2)$, $a = q, g$, unintegrated over the transverse momentum q_T, are calculated from auxiliary functions $h_a(x, q_T^2)$, which satisfy single-scale evolution equations.
- An advantage of the single-scale unified BFKL/DGLAP equation is that it incorporates a major part of the subleading order $\ln(1/x)$ (BFKL) effects.

$$\Phi_g(x, q_T^2, \mu^2) = T_g(q_T, \mu) \frac{\alpha_s(q_T^2)}{2\pi} \times$$
$$\times \quad \left(\int_x^{\mu/(\mu+q_T)} dz \int^{q_T^2} \frac{dk_T^2}{k_T^2} \left[\bar{P}(z) h_g(x/z, k_T^2) + P_{gq}(z) \sum h_q(x/z, k_T^2) \right] + \right.$$
$$+ \quad \left. 2N_c \int_x^{\mu/(\mu+k_T)} \frac{dz}{z} \int \frac{d^2p}{\pi p^2} \left[\frac{q_T^2}{k_T^2} h_g(x/z, k_T^2) - \theta(q_T^2 - p^2) h_g(x/z, q_T^2) \right] \right),$$

$$T_g(q_T, \mu) = \exp\left(- \int_{q_T^2}^{\mu^2} \frac{\alpha_s(k_T^2)}{2\pi} \frac{dk_T^2}{k_T^2} \sum_a \int_0^{1-\Delta} P_{ag}(z) dz \right),$$
$$\bar{P}(z) = P_{gg}(z) - 2N_c/z.$$

Unintegrated gluon distribution functions: KMR prescription.

- The formalism embodies both DGLAP and BFKL contributions.
- The key observation is that the μ dependence of the unintegrated distributions enters at the last step of the evolution, so single-scale evolution equations can be used.
- The parton distributions $\Phi_a^h(x, q_T^2, \mu^2)$, $a = q, g$, unintegrated over the transverse momentum q_T, are calculated from auxiliary functions $h_a(x, q_T^2)$, which satisfy single-scale evolution equations.
- An advantage of the single-scale unified BFKL/DGLAP equation is that it incorporates a major part of the subleading order $\ln(1/x)$ (BFKL) effects.

$$\Phi_g(x, q_T^2, \mu^2) = T_g(q_T, \mu)\frac{\alpha_S(q_T^2)}{2\pi} \times$$

$$\times \quad \left(\int_x^{\mu/(\mu+q_T)} dz \int^{q_T^2} \frac{dk_T^2}{k_T^2}\left[\bar{P}(z)h_g(x/z, k_T^2) + P_{gq}(z)\sum h_q(x/z, k_T^2)\right] + \right.$$

$$\left. + \quad 2N_c \int_x^{\mu/(\mu+k_T)} \frac{dz}{z} \int \frac{d^2p}{\pi p^2}\left[\frac{q_T^2}{k_T^2}h_g(x/z, k_T^2) - \theta(q_T^2 - p^2)h_g(x/z, q_T^2)\right]\right),$$

$$T_g(q_T, \mu) \quad = \quad \exp\left(-\int_{q_T^2}^{\mu^2} \frac{\alpha_S(k_T^2)}{2\pi}\frac{dk_T^2}{k_T^2}\sum_a \int_0^{1-\Delta} P_{ag}(z)dz\right),$$

$$\bar{P}(z) \quad = \quad P_{gg}(z) - 2N_c/z.$$

Unintegrated gluon distribution functions: KMR prescription.

- The formalism embodies both DGLAP and BFKL contributions.
- The key observation is that the μ dependence of the unintegrated distributions enters at the last step of the evolution, so single-scale evolution equations can be used.
- The parton distributions $\Phi_a^h(x, q_T^2, \mu^2)$, $a = q, g$, unintegrated over the transverse momentum q_T, are calculated from auxiliary functions $h_a(x, q_T^2)$, which satisfy single-scale evolution equations.
- An advantage of the single-scale unified BFKL/DGLAP equation is that it incorporates a major part of the subleading order $\ln(1/x)$ (BFKL) effects.

$$\Phi_g(x, q_T^2, \mu^2) = T_g(q_T, \mu) \frac{\alpha_S(q_T^2)}{2\pi} \times$$
$$\times \quad \left(\int_x^{\mu/(\mu+q_T)} dz \int^{q_T^2} \frac{dk_T^2}{k_T^2} \left[\bar{P}(z) h_g(x/z, k_T^2) + P_{gq}(z) \sum h_q(x/z, k_T^2) \right] + \right.$$
$$\left. + \quad 2N_c \int_x^{\mu/(\mu+k_T)} \frac{dz}{z} \int \frac{d^2p}{\pi p^2} \left[\frac{q_T^2}{k_T^2} h_g(x/z, k_T^2) - \theta(q_T^2 - p^2) h_g(x/z, q_T^2) \right] \right),$$

$$T_g(q_T, \mu) = \exp\left(- \int_{q_T^2}^{\mu^2} \frac{\alpha_S(k_T^2)}{2\pi} \frac{dk_T^2}{k_T^2} \sum_a \int_0^{1-\Delta} P_{ag}(z) dz \right),$$
$$\bar{P}(z) = P_{gg}(z) - 2N_c/z.$$

Unintegrated gluon distribution functions: KMR prescription.

- The formalism embodies both DGLAP and BFKL contributions.
- The key observation is that the μ dependence of the unintegrated distributions enters at the last step of the evolution, so single-scale evolution equations can be used.
- The parton distributions $\Phi_a^h(x, q_T^2, \mu^2)$, $a = q, g$, unintegrated over the transverse momentum q_T, are calculated from auxiliary functions $h_a(x, q_T^2)$, which satisfy single-scale evolution equations.
- An advantage of the single-scale unified BFKL/DGLAP equation is that it incorporates a major part of the subleading order $\ln(1/x)$ (BFKL) effects.

$$\Phi_g(x, q_T^2, \mu^2) = T_g(q_T, \mu) \frac{\alpha_s(q_T^2)}{2\pi} \times$$

$$\times \quad \left(\int_x^{\mu/(\mu+q_T)} dz \int^{q_T^2} \frac{dk_T^2}{k_T^2} \left[\bar{P}(z) h_g(x/z, k_T^2) + P_{gq}(z) \sum h_q(x/z, k_T^2) \right] + \right.$$

$$+ \quad \left. 2N_c \int_x^{\mu/(\mu+k_T)} \frac{dz}{z} \int \frac{d^2p}{\pi p^2} \left[\frac{q_T^2}{k_T^2} h_g(x/z, k_T^2) - \theta(q_T^2 - p^2) h_g(x/z, q_T^2) \right] \right),$$

$$T_g(q_T, \mu) = \exp\left(- \int_{q_T^2}^{\mu^2} \frac{\alpha_s(k_T^2)}{2\pi} \frac{dk_T^2}{k_T^2} \sum_a \int_0^{1-\Delta} P_{ag}(z) dz \right),$$

$$\bar{P}(z) = P_{gg}(z) - 2N_c/z.$$

Hard scattering matrix elements

k_T-factorization approach (KFA)
polarization vector of initial-state gluon with 4-momentum $k = (k_0, \mathbf{k_T}, k_z)$:
$\epsilon^\mu(k) = \frac{k_T^\mu}{|\mathbf{k_T}|} \Rightarrow$ no gauge-invariance in the case of gluons in final state; no generally accepted prescription for the treatment of off-shell initial-state quarks.

Parton Reggeization Approach (PRA)
KFA with *Reggeized* initial-state partons

Hard scattering matrix elements

k_T-factorization approach (KFA)
polarization vector of initial-state gluon with 4-momentum $k = (k_0, \mathbf{k_T}, k_z)$:
$\epsilon^\mu(k) = \frac{k_T^\mu}{|\mathbf{k_T}|} \Rightarrow$ no gauge-invariance in the case of gluons in final state; no generally accepted prescription for the treatment of off-shell initial-state quarks.

Parton Reggeization Approach (PRA)
KFA with *Reggeized* initial-state partons

Parton Reggeization Approach

The Regge limit of QCD: the center-of-mass energy is large $\sqrt{S} \to \infty$ and the momentum transfer $\sqrt{-t}$ is fixed

We propose the c.m. energy of LHC $\sqrt{S} = 7$ TeV to be large enough, and the finiteness of t is controlled by fixed p_T of final jets.

The most appropriate approach for the description of scattering amplitudes is given by the theory of complex angular momenta (Gribov-Regge theory)

The Regge kinematics is a particular case of **multi-Regge kinematics (MRK)**. MRK is the kinematics where all particles have limited (not growing with s) transverse momenta and are combined into jets with limited invariant mass of each jet and large (growing with s) invariant masses of any pair of the jets. The MRK gives dominant contributions to cross sections of QCD processes at high energy.

Parton Reggeization Approach

The Regge limit of QCD: the center-of-mass energy is large $\sqrt{S} \to \infty$ and the momentum transfer $\sqrt{-t}$ is fixed
We propose the c.m. energy of LHC $\sqrt{S} = 7$ TeV to be large enough, and the finiteness of t is controlled by fixed p_T of final jets.

The most appropriate approach for the description of scattering amplitudes is given by the theory of complex angular momenta (Gribov-Regge theory)

The Regge kinematics is a particular case of **multi-Regge kinematics (MRK)**. MRK is the kinematics where all particles have limited (not growing with s) transverse momenta and are combined into jets with limited invariant mass of each jet and large (growing with s) invariant masses of any pair of the jets. The MRK gives dominant contributions to cross sections of QCD processes at high energy.

Parton Reggeization Approach

The Regge limit of QCD: the center-of-mass energy is large $\sqrt{S} \to \infty$ and the momentum transfer $\sqrt{-t}$ is fixed
We propose the c.m. energy of LHC $\sqrt{S} = 7$ TeV to be large enough, and the finiteness of t is controlled by fixed p_T of final jets.

The most appropriate approach for the description of scattering amplitudes is given by the theory of complex angular momenta (Gribov-Regge theory)

The Regge kinematics is a particular case of **multi-Regge kinematics (MRK)**. MRK is the kinematics where all particles have limited (not growing with s) transverse momenta and are combined into jets with limited invariant mass of each jet and large (growing with s) invariant masses of any pair of the jets. The MRK gives dominant contributions to cross sections of QCD processes at high energy.

Parton Reggeization Approach

The Regge limit of QCD**: the center-of-mass energy is large $\sqrt{S} \to \infty$ and the momentum transfer $\sqrt{-t}$ is fixed**
We propose the c.m. energy of LHC $\sqrt{S} = 7$ TeV to be large enough, and the finiteness of t is controlled by fixed p_T of final jets.

The most appropriate approach for the description of scattering amplitudes is given by the theory of complex angular momenta (Gribov-Regge theory)

The Regge kinematics is a particular case of **multi-Regge kinematics (MRK)**. MRK is the kinematics where all particles have limited (not growing with s) transverse momenta and are combined into jets with limited invariant mass of each jet and large (growing with s) invariant masses of any pair of the jets. The MRK gives dominant contributions to cross sections of QCD processes at high energy.

Parton Reggeization Approach: multi-Regge kinematics

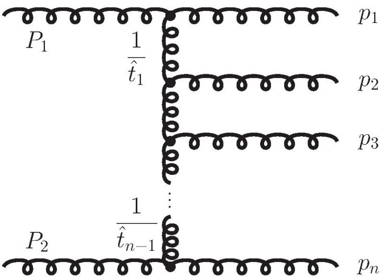

$$p_i = \beta_i P_1 + \alpha_i P_2 + p_{iT}$$
$$S = (P_1 + P_2)^2$$
$$S\alpha_i\beta_i = p_i^2 - p_{iT}^2$$
$$1/S \sim \beta_{n+1} \ll \beta_n \ll ... \ll \beta_0 \sim 1$$
$$1/S \sim \alpha_0 \ll \alpha_1 \ll ... \ll \alpha_{n+1} \sim 1$$
$$S_i = (p_{i-1} + p_i)^2 = S\beta_{i-1}\alpha_i$$
$$S_i \gg |p_{iT}^2| \sim |t_i| = |q_i^2|$$

Despite of a great number of contributing Feynman diagrams it turns out that at the Born level in the MRK amplitudes acquire a simple factorized form. In the leading logarithmic approximation (LLA) the n-gluon production amplitude in this kinematics has the multi-Regge form

$$A_{2+n}^{LLA} = A_{2+n}^{tree} \prod_{i=1}^{n+1} s_i^{\omega(t_i)}$$

Radiative corrections to these amplitudes do not destroy this form, and their energy dependence is given by Regge factors $s_i^{\omega(t_i)}$. This phenomenon is called **gluon Reggeization**.

Parton Reggeization Approach: multi-Regge kinematics

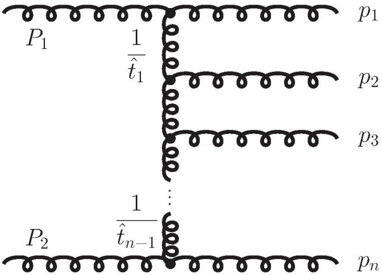

$$p_i = \beta_i P_1 + \alpha_i P_2 + p_{iT}$$
$$S = (P_1 + P_2)^2$$
$$S\alpha_i\beta_i = p_i^2 - p_{iT}^2$$
$$1/S \sim \beta_{n+1} \ll \beta_n \ll \ldots \ll \beta_0 \sim 1$$
$$1/S \sim \alpha_0 \ll \alpha_1 \ll \ldots \ll \alpha_{n+1} \sim 1$$
$$S_i = (p_{i-1} + p_i)^2 = S\beta_{i-1}\alpha_i$$
$$S_i \gg |p_{iT}^2| \sim |t_i| = |q_i^2|$$

Despite of a great number of contributing Feynman diagrams it turns out that at the Born level in the MRK amplitudes acquire a simple factorized form. In the leading logarithmic approximation (LLA) the n-gluon production amplitude in this kinematics has the multi-Regge form

$$A_{2+n}^{LLA} = A_{2+n}^{tree} \prod_{i=1}^{n+1} s_i^{\omega(t_i)}$$

Radiative corrections to these amplitudes do not destroy this form, and their energy dependence is given by Regge factors $s_i^{\omega(t_i)}$. This phenomenon is called **gluon Reggeization**.

Particle Reggeization

The gluons in each crossing channel t_i are Reggeized if one takes into account the radiative corrections to the Born production amplitude A^{tree}_{2+n}.

The production amplitude in the tree approximation has the factorised form:

$$A^{tree}_{2+n} = 2Sg_s T^{c_1}_{AA'} \Gamma_{A'A} \frac{1}{t_1} g_s T^{d_1}_{c_2 c_1} \Gamma^1_{21} \frac{1}{t_2} \dots g_s T^{d_n}_{c_{n+1} c_n} \Gamma^n_{n+1,n} \frac{1}{t_{n+1}} g_s T^{c_{n+1}}_{B'B} \Gamma_{B'B},$$

$\Gamma^r_{r+1,r}$ – Reggeon-Reggeon-particle (RRP) vertex,
$\Gamma_{AA'}$ – Reggeon-particle-particle (RPP) vertex.

The effect of particle Reggeization was discovered in QED in 1964:
M. Gell-Mann, M. L. Goldberger, F. E. Low, E. Marx, and F. Zachariasen, Phys.Rev. ***133****, B161-B174 (1964).*

The gluon Reggeization in QCD:
E. A. Kuraev, L. N. Lipatov, and V. S. Fadin, Sov. Phys. JETP ***44****, 443 (1976)*
I. I. Balitsky and L. N. Lipatov, Sov. J. Nucl. Phys. ***28****, 822 (1978)*

The quark Reggeization in QCD:
V. S. Fadin and V. E. Sherman, JETP Lett. ***23****, 599 (1976)*

Particle Reggeization

The gluons in each crossing channel t_i are Reggeized if one takes into account the radiative corrections to the Born production amplitude A^{tree}_{2+n}.

The production amplitude in the tree approximation has the factorised form:

$$A^{tree}_{2+n} = 2Sg_s T^{c_1}_{AA'} \Gamma_{A'A} \frac{1}{t_1} g_s T^{d_1}_{c_2 c_1} \Gamma^1_{21} \frac{1}{t_2} \ldots g_s T^{d_n}_{c_{n+1} c_n} \Gamma^n_{n+1,n} \frac{1}{t_{n+1}} g_s T^{c_{n+1}}_{B'B} \Gamma_{B'B},$$

$\Gamma^r_{r+1,r}$ – Reggeon-Reggeon-particle (RRP) vertex,
$\Gamma_{AA'}$ – Reggeon-particle-particle (RPP) vertex.

The effect of particle Reggeization was discovered in QED in 1964:
M. Gell-Mann, M. L. Goldberger, F. E. Low, E. Marx, and F. Zachariasen, Phys.Rev. ***133****, B161-B174 (1964).*

The gluon Reggeization in QCD:
E. A. Kuraev, L. N. Lipatov, and V. S. Fadin, Sov. Phys. JETP ***44****, 443 (1976)*
I. I. Balitsky and L. N. Lipatov, Sov. J. Nucl. Phys. ***28****, 822 (1978)*

The quark Reggeization in QCD:
V. S. Fadin and V. E. Sherman, JETP Lett. ***23****, 599 (1976)*

Particle Reggeization

The gluons in each crossing channel t_i are Reggeized if one takes into account the radiative corrections to the Born production amplitude A^{tree}_{2+n}.

The production amplitude in the tree approximation has the factorised form:

$$A^{tree}_{2+n} = 2Sg_s T^{c_1}_{AA'} \Gamma_{A'A} \frac{1}{t_1} g_s T^{d_1}_{c_2 c_1} \Gamma^1_{21} \frac{1}{t_2} \dots g_s T^{d_n}_{c_{n+1} c_n} \Gamma^n_{n+1,n} \frac{1}{t_{n+1}} g_s T^{c_{n+1}}_{B'B} \Gamma_{B'B},$$

$\Gamma^r_{r+1,r}$ – Reggeon-Reggeon-particle (RRP) vertex,
$\Gamma_{AA'}$ – Reggeon-particle-particle (RPP) vertex.

The effect of particle Reggeization was discovered in QED in 1964:
M. Gell-Mann, M. L. Goldberger, F. E. Low, E. Marx, and F. Zachariasen, Phys.Rev. ***133****, B161-B174 (1964).*

The gluon Reggeization in QCD:
E. A. Kuraev, L. N. Lipatov, and V. S. Fadin, Sov. Phys. JETP ***44****, 443 (1976)*
I. I. Balitsky and L. N. Lipatov, Sov. J. Nucl. Phys. ***28****, 822 (1978)*

The quark Reggeization in QCD:
V. S. Fadin and V. E. Sherman, JETP Lett. ***23****, 599 (1976)*

Parton Reggeization Approach: effective vertices

There are **two ways to derive effective vertices**:

- From the analyticity and unitarity constraints for multiparticle production amplitudes. These methods were developed in the works of Lipatov, Fadin, Kuraev and co-authors.
- From the Lagrangian of non-Abelian gauge invariant effective theory, which includes fields of Reggeized particles, firstly written down in *L. N. Lipatov, Nucl. Phys.* ***B452****, 369 (1995).*

The set of Feynman rules for Reggeized particles interactions was derived and presented in the works:
E. N. Antonov, L. N. Lipatov, E. A. Kuraev, and I. O. Cherednikov, Nucl. Phys. ***B721****, 111 (2005)*
L. N. Lipatov and M. I. Vyazovsky, Nucl. Phys. ***B597****, 399 (2001).*

Parton Reggeization Approach: effective vertices

There are **two ways to derive effective vertices**:

- From the analyticity and unitarity constraints for multiparticle production amplitudes. These methods were developed in the works of Lipatov, Fadin, Kuraev and co-authors.
- From the Lagrangian of non-Abelian gauge invariant effective theory, which includes fields of Reggeized particles, firstly written down in *L. N. Lipatov, Nucl. Phys.* ***B452****, 369 (1995).*

The set of Feynman rules for Reggeized particles interactions was derived and presented in the works:
E. N. Antonov, L. N. Lipatov, E. A. Kuraev, and I. O. Cherednikov, Nucl. Phys. ***B721****, 111 (2005)*
L. N. Lipatov and M. I. Vyazovsky, Nucl. Phys. ***B597****, 399 (2001).*

Parton Reggeization Approach: effective vertices

There are **two ways to derive effective vertices**:

- From the analyticity and unitarity constraints for multiparticle production amplitudes. These methods were developed in the works of Lipatov, Fadin, Kuraev and co-authors.
- From the Lagrangian of non-Abelian gauge invariant effective theory, which includes fields of Reggeized particles, firstly written down in *L. N. Lipatov, Nucl. Phys.* ***B452****, 369 (1995)*.

The set of Feynman rules for Reggeized particles interactions was derived and presented in the works:
E. N. Antonov, L. N. Lipatov, E. A. Kuraev, and I. O. Cherednikov, Nucl. Phys. ***B721****, 111 (2005)*
L. N. Lipatov and M. I. Vyazovsky, Nucl. Phys. ***B597****, 399 (2001)*.

Parton Reggeization Approach: effective vertices

There are **two ways to derive effective vertices**:

- From the analyticity and unitarity constraints for multiparticle production amplitudes. These methods were developed in the works of Lipatov, Fadin, Kuraev and co-authors.
- From the Lagrangian of non-Abelian gauge invariant effective theory, which includes fields of Reggeized particles, firstly written down in *L. N. Lipatov, Nucl. Phys.* ***B452****, 369 (1995)*.

The set of Feynman rules for Reggeized particles interactions was derived and presented in the works:
E. N. Antonov, L. N. Lipatov, E. A. Kuraev, and I. O. Cherednikov, Nucl. Phys. ***B721****, 111 (2005)*
L. N. Lipatov and M. I. Vyazovsky, Nucl. Phys. ***B597****, 399 (2001)*.

Parton Reggeization Approach: application

Since 1970-s until now the strong mathematical apparatus concerning parton Reggeization was developed and in 2011 was extended to the gravity.
We are aim to apply this model to the description of real processes. The reasons are:

- To obtain the agreement with experimental data one needs to perform the pQCD calculations in NLO order and higher $\Rightarrow$ much time and computational resources are involved.
- Just at the Tevatron and certainly at the LHC $S \gg \mu^2$, $\mu \sim m_T \approx p_T$. So we enter in the region of small $x \simeq \mu/\sqrt{S}$ and large logarithms of type $\ln^n(1/x)$ arise violating the convergence of pQCD series in α_s.

These large logarithms $\ln^n(1/x)$ are resummed by Balitsky-Fadin-Kuraev-Lipatov (BFKL) evolution equation for non-integrated over transverse parton distribution functions (PDFs). The gluon Reggeization is the basis of BFKL approach.

Parton Reggeization Approach: application

Since 1970-s until now the strong mathematical apparatus concerning parton Reggeization was developed and in 2011 was extended to the gravity.
We are aim to apply this model to the description of real processes. The reasons are:

- To obtain the agreement with experimental data one needs to perform the pQCD calculations in NLO order and higher $\Rightarrow$ much time and computational resources are involved.
- Just at the Tevatron and certainly at the LHC $S \gg \mu^2$, $\mu \sim m_T \approx p_T$. So we enter in the region of small $x \simeq \mu/\sqrt{S}$ and large logarithms of type $\ln^n(1/x)$ arise violating the convergence of pQCD series in α_S.

These large logarithms $\ln^n(1/x)$ are resummed by Balitsky-Fadin-Kuraev-Lipatov (BFKL) evolution equation for non-integrated over transverse parton distribution functions (PDFs). The gluon Reggeization is the basis of BFKL approach.

Parton Reggeization Approach: application

Since 1970-s until now the strong mathematical apparatus concerning parton Reggeization was developed and in 2011 was extended to the gravity.
We are aim to apply this model to the description of real processes. The reasons are:

- To obtain the agreement with experimental data one needs to perform the pQCD calculations in NLO order and higher $\Rightarrow$ much time and computational resources are involved.
- Just at the Tevatron and certainly at the LHC $S \gg \mu^2$, $\mu \sim m_T \approx p_T$. So we enter in the region of small $x \simeq \mu/\sqrt{S}$ and large logarithms of type $\ln^n(1/x)$ arise violating the convergence of pQCD series in α_s.

These large logarithms $\ln^n(1/x)$ are resummed by Balitsky-Fadin-Kuraev-Lipatov (BFKL) evolution equation for non-integrated over transverse parton distribution functions (PDFs). The gluon Reggeization is the basis of BFKL approach.

Parton Reggeization Approach: application

Since 1970-s until now the strong mathematical apparatus concerning parton Reggeization was developed and in 2011 was extended to the gravity.
We are aim to apply this model to the description of real processes. The reasons are:

- To obtain the agreement with experimental data one needs to perform the pQCD calculations in NLO order and higher $\Rightarrow$ much time and computational resources are involved.
- Just at the Tevatron and certainly at the LHC $S \gg \mu^2$, $\mu \sim m_T \approx p_T$. So we enter in the region of small $x \simeq \mu/\sqrt{S}$ and large logarithms of type $\ln^n(1/x)$ arise violating the convergence of pQCD series in α_s.

These large logarithms $\ln^n(1/x)$ are resummed by Balitsky-Fadin-Kuraev-Lipatov (BFKL) evolution equation for non-integrated over transverse parton distribution functions (PDFs). The gluon Reggeization is the basis of BFKL approach.

Parton Reggeization Approach: the factorization hypothesis

In the leading order of PRA the hypothesis of factorization of the effects of long and short distances is proved:

$$d\sigma(p+p\to\mathcal{H}+X,S)=\int\frac{dx_1}{x_1}\int d|\mathbf{q}_{1T}|^2\int\frac{d\varphi_1}{2\pi}\Phi(x_1,|\mathbf{q}_{1T}|^2,\mu^2)$$
$$\times\int\frac{dx_2}{x_2}\int d|\mathbf{q}_{2T}|^2\int\frac{d\varphi_2}{2\pi}\Phi(x_2,|\mathbf{q}_{2T}|^2,\mu^2)$$
$$\times d\hat\sigma(R+R\to\mathcal{H}+X,\mathbf{q}_{1T},\mathbf{q}_{2T},\hat s),$$

Dijet production in QMRK

The production of gluon pairs with close rapidities in the central region whereas the protons remnants have large modula of rapidities satisfies the conditions of quasi-multi-Regge kinematics (QMRK). MRK is a particular case of QMRK.

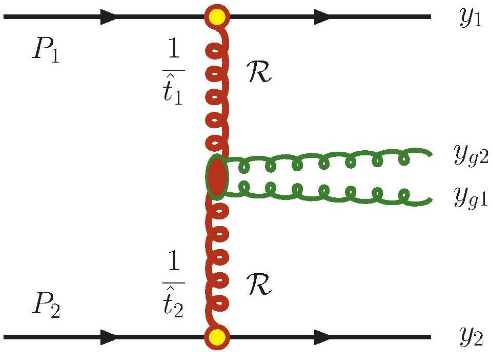

Figure 1 : QMRK: $y_1 \ll y_{g1} \simeq y_{g2} \ll y_2$

Dijet production: the hard subprocesses

The full number of hard subprocesses in QMRK contributing to dijet production:

$$
\begin{aligned}
R+R &\to g+g,\\
R+R &\to q+\bar{q},\\
Q+R &\to q+g,\\
Q+Q &\to q+q,\\
Q+Q' &\to q+q',\\
Q+\bar{Q} &\to q+\bar{q},\\
Q+\bar{Q} &\to q'+\bar{q}',\\
Q+\bar{Q} &\to g+g.
\end{aligned}
$$

At the LHC the dominant partonic subprocess is:

$$\mathcal{R}(q_1)+\mathcal{R}(q_2)\to g(k_1)+g(k_2)$$

$q_i^\mu = x_i P_i^\mu + q_{iT}^\mu$ $(i=1,2)$ – four-momenta of the Reggeized gluons;
$P_{1,2}^\mu = (\sqrt{S}/2)(1,0,0,\pm 1)$ – four-momenta of the incoming protons;
$q_{iT}^\mu = (0,\mathbf{q}_{iT},0)$, $t_i = -q_{iT}^2 = \mathbf{q}_{iT}^2$.
$k_{1,2}$ – four-momenta of the final gluons, $k_1^2 = k_2^2 = 0$.

Dijet production: the hard subprocesses

The full number of hard subprocesses in QMRK contributing to dijet production:

$$\begin{aligned}
R + R &\to g + g, \\
R + R &\to q + \bar{q}, \\
Q + R &\to q + g, \\
Q + Q &\to q + q, \\
Q + Q' &\to q + q', \\
Q + \bar{Q} &\to q + \bar{q}, \\
Q + \bar{Q} &\to q' + \bar{q}', \\
Q + \bar{Q} &\to g + g.
\end{aligned}$$

At the LHC the dominant partonic subprocess is:

$$\mathcal{R}(q_1) + \mathcal{R}(q_2) \to g(k_1) + g(k_2)$$

$q_i^\mu = x_i P_i^\mu + q_{iT}^\mu$ $(i = 1, 2)$ – four-momenta of the Reggeized gluons;
$P_{1,2}^\mu = (\sqrt{S}/2)(1, 0, 0, \pm 1)$ – four-momenta of the incoming protons;
$q_{iT}^\mu = (0, \mathbf{q}_{iT}, 0)$, $t_i = -q_{iT}^2 = \mathbf{q}_{iT}^2$.
$k_{1,2}$ – four-momenta of the final gluons, $k_1^2 = k_2^2 = 0$.

Dijet production: the hard subprocesses

The effective $\mathcal{RR}gg$ vertex

$$C^{gg,\ cd,\ \mu\nu}_{RR,ab}(q_1,q_2,k_1,k_2) = g_s^2\frac{q_1^+ q_2^-}{4\sqrt{t_1 t_2}}\times$$

$$\times\Big(T_1 s^{-1}\Gamma^{(+-)\sigma}(q_1,q_2)\gamma_{\mu\nu\sigma}(-k_1,-k_2)+$$

$$+T_3 t^{-1}\Gamma^{\sigma\mu-}(q_1,k_1-q_1)\Gamma^{\sigma\nu+}(k_2-q_2,q_2)-$$

$$-T_2 u^{-1}\Gamma^{\sigma\nu-}(q_1,k_2-q_1)\Gamma^{\sigma\mu+}(k_1-q_2,q_2)-$$

$$-T_1(n^-_\mu n^+_\nu - n^-_\nu n^+_\mu) - T_2(2g_{\mu\nu}-n^-_\mu n^+_\nu) - T_3(-2g_{\mu\nu}+n^-_\nu n^+_\mu)+$$

$$+\Delta^{\mu\nu+}(q_1,q_2,k_1,k_2)+\Delta^{\mu\nu-}(q_1,q_2,k_1,k_2)\Big)$$

$$T_1 = f_{cdr}f_{abr},\quad T_2 = f_{dar}f_{cbr},\quad T_3 = f_{acr}f_{dbr},\quad T_1+T_2+T_3=0$$

$$\Delta^{\mu\nu+}(q_1,q_2,k_1,k_2) = 2t_2 n^+_\mu n^+_\nu\left(\frac{T_3}{k_2^+ q_1^+}-\frac{T_2}{k_1^+ q_1^+}\right),$$

$$\Delta^{\mu\nu-}(q_1,q_2,k_1,k_2) = 2t_1 n^-_\mu n^-_\nu\left(\frac{T_3}{k_1^- q_2^-}-\frac{T_2}{k_2^- q_2^-}\right)$$

The light-cone vectors $n^+ = 2P_2/\sqrt{S}$ and $n^- = 2P_1/\sqrt{S}$, $k^\pm = k\cdot n^\pm$ for any four-vector k^μ.

Dijet production: the hard subprocesses

The effective $\mathcal{RR}gg$ vertex

$$C^{gg,\ cd,\ \mu\nu}_{RR,ab}(q_1,q_2,k_1,k_2) = g_s^2\frac{q_1^+q_2^-}{4\sqrt{t_1t_2}}\times$$
$$\times\Big(T_1 s^{-1}\Gamma^{(+-)\sigma}(q_1,q_2)\gamma_{\mu\nu\sigma}(-k_1,-k_2)+$$
$$+T_3t^{-1}\Gamma^{\sigma\mu-}(q_1,k_1-q_1)\Gamma^{\sigma\nu+}(k_2-q_2,q_2)-$$
$$-T_2u^{-1}\Gamma^{\sigma\nu-}(q_1,k_2-q_1)\Gamma^{\sigma\mu+}(k_1-q_2,q_2)-$$
$$-T_1(n_\mu^-n_\nu^+-n_\nu^-n_\mu^+)-T_2(2g_{\mu\nu}-n_\mu^-n_\nu^+)-T_3(-2g_{\mu\nu}+n_\nu^-n_\mu^+)+$$
$$+\Delta^{\mu\nu+}(q_1,q_2,k_1,k_2)+\Delta^{\mu\nu-}(q_1,q_2,k_1,k_2)\Big)$$

$$T_1=f_{cdr}f_{abr},\quad T_2=f_{dar}f_{cbr},\quad T_3=f_{acr}f_{dbr},\quad T_1+T_2+T_3=0$$
$$\Delta^{\mu\nu+}(q_1,q_2,k_1,k_2)=2t_2n_\mu^+n_\nu^+\left(\frac{T_3}{k_2^+q_1^+}-\frac{T_2}{k_1^+q_1^+}\right),$$
$$\Delta^{\mu\nu-}(q_1,q_2,k_1,k_2)=2t_1n_\mu^-n_\nu^-\left(\frac{T_3}{k_1^-q_2^-}-\frac{T_2}{k_2^-q_2^-}\right)$$

The light-cone vectors $n^+=2P_2/\sqrt{S}$ and $n^-=2P_1/\sqrt{S}$, $k^\pm=k\cdot n^\pm$ for any four-vector k^μ.

Dijet production: the hard subprocesses

The effective $\mathcal{RR}gg$ vertex

$$C^{gg,\ cd,\ \mu\nu}_{RR,ab}(q_1,q_2,k_1,k_2) = g_s^2 \frac{q_1^+ q_2^-}{4\sqrt{t_1 t_2}} \times$$
$$\times \Big(T_1 s^{-1} \Gamma^{(+-)\sigma}(q_1,q_2)\gamma_{\mu\nu\sigma}(-k_1,-k_2) +$$
$$+T_3 t^{-1}\Gamma^{\sigma\mu -}(q_1,k_1-q_1)\Gamma^{\sigma\nu +}(k_2-q_2,q_2) -$$
$$-T_2 u^{-1}\Gamma^{\sigma\nu -}(q_1,k_2-q_1)\Gamma^{\sigma\mu +}(k_1-q_2,q_2) -$$
$$-T_1(n_\mu^- n_\nu^+ - n_\nu^- n_\mu^+) - T_2(2g_{\mu\nu} - n_\mu^- n_\nu^+) - T_3(-2g_{\mu\nu} + n_\nu^- n_\mu^+) +$$
$$+\Delta^{\mu\nu +}(q_1,q_2,k_1,k_2) + \Delta^{\mu\nu -}(q_1,q_2,k_1,k_2) \Big)$$

$$T_1 = f_{cdr} f_{abr}, \quad T_2 = f_{dar} f_{cbr}, \quad T_3 = f_{acr} f_{dbr}, \quad T_1 + T_2 + T_3 = 0$$
$$\Delta^{\mu\nu +}(q_1,q_2,k_1,k_2) = 2t_2 n_\mu^+ n_\nu^+ \left(\frac{T_3}{k_2^+ q_1^+} - \frac{T_2}{k_1^+ q_1^+} \right),$$
$$\Delta^{\mu\nu -}(q_1,q_2,k_1,k_2) = 2t_1 n_\mu^- n_\nu^- \left(\frac{T_3}{k_1^- q_2^-} - \frac{T_2}{k_2^- q_2^-} \right)$$

The light-cone vectors $n^+ = 2P_2/\sqrt{S}$ and $n^- = 2P_1/\sqrt{S}$, $k^\pm = k \cdot n^\pm$ for any four-vector k^μ.

The matrix element of subprocess $\mathcal{RR} \to gg$

The general form of the squared amplitudes for all subprocesses

$$\overline{|\mathcal{M}|^2} = \pi^2 \alpha_S^2 A \sum_{n=0}^{4} W_n S^n,$$

For the subprocess $\mathcal{RR} \to gg$:

$$\begin{aligned}
A &= \frac{18}{a_1 a_2 b_1 b_2 s^2 t^2 u^2 t_1 t_2},\\
W_0 &= x_1 x_2 s^2 t u t_1 t_2 \left(x_1 x_2 (tu + t_1 t_2) + (a_1 b_2 + a_2 b_1) tu\right),\\
W_1 &= x_1 x_2 s t_1 t_2 \left[t^2 u \left(a_1 b_2 (a_2 b_2 + a_1 x_2)(t_1 + t_2) - a_2 b_1 (a_1 b_1 t_1 + a_2 b_2 t_2) + \right.\right.\\
&+ \left.\left. (x_2 (a_1^2 b_2 + a_2^2 b_1) + a_1 a_2 (b_1 - b_2)^2) u + x_1 x_2 a_1 b_2 t \right) \right] +\\
&+ \left[a_1 \leftrightarrow a_2, b_1 \leftrightarrow b_2, t \leftrightarrow u \right],\\
W_2 &= a_1 a_2 b_1 b_2 t u \left(x_1^2 x_2^2 \left[2(t_1 + t_2)(t^2 u + t_1 t_2 (s + u - t)) + \right.\right.\\
&+ \left. t u ((t_1 - t_2)^2 + t(u + 2t)) \right] +\\
&+ x_1 x_2 t t_1 t_2 (4(x_1 b_1 + x_2 a_2)(s + u) - (a_1 b_1 + a_2 b_2) u) +\\
&+ \left. t u (x_1^2 b_2 (2 x_2 t - b_1 t_1) t_1 + x_2^2 a_1 (2 x_1 t - a_2 t_2) t_2) \right) +\\
&+ \left(a_1 \leftrightarrow a_2, b_1 \leftrightarrow b_2, t \leftrightarrow u \right),
\end{aligned}$$

The matrix element of subprocess $\mathcal{R}\mathcal{R} \to gg$

$$
\begin{aligned}
W_3 &= x_1 x_2 a_1 a_2 b_1 b_2 \Big[t^2 u \Big(2a_1 b_2 (x_1 x_2 (t_1 + t_2)(2t - u - s) - (x_1 b_2 t_1 + x_2 a_1 t_2)(u + s)) + \\
&+ [x_1 t_1 (2(a_1 b_2^2 + a_2 b_1^2) + 3x_1 b_1 b_2) + x_2 t_2 (2(a_1^2 b_2 + a_2^2 b_1) + 3a_1 a_2 x_2)] u + \\
&+ 4x_1 x_2 t ((a_1 b_2 + a_2 b_1) u + a_1 b_2 t) \Big) \Big] + \Big[a_1 \leftrightarrow a_2, b_1 \leftrightarrow b_2, t \leftrightarrow u \Big], \\
W_4 &= x_1^2 x_2^2 a_1 a_2 b_1 b_2 \Big[t \Big(a_1 a_2 b_1 b_2 u (t_1 + t_2)(t - u - s) + (a_1 b_2 + a_2 b_1)^2 t u^2 - \\
&- 2a_1 b_2 t (s + u)(2a_2 b_1 u - a_1 b_2 s) \Big) \Big] + \Big[a_1 \leftrightarrow a_2, b_1 \leftrightarrow b_2, t \leftrightarrow u \Big].
\end{aligned}
$$

The invariant variables: $s = (q_1 + q_2)^2$, $t = (q_1 - k_1)^2$, $u = (q_1 - k_2)^2$, $a_1 = 2k_1 \cdot P_2/S$, $a_2 = 2k_2 \cdot P_2/S$, $b_1 = 2k_1 \cdot P_1/S$, $b_2 = 2k_2 \cdot P_1/S$.

The amplitudes and squared matrix elements for the full set of $2 \to 2$ subprocesses with Reggeons in the initial state which give contribution to dijet production are presented in the work *M.A. Nefedov, V.A. Saleev, A. V Shipilova.* Dijet azimuthal decorrelations at the LHC in the parton Reggeization approach. Phys. Rev. D**87** (2013) 094030. The all squared matrix elements are checked to give the correct expressions in the Parton Model limit.

The matrix element of subprocess $\mathcal{RR} \to gg$

$$
\begin{aligned}
W_3 &= x_1 x_2 a_1 a_2 b_1 b_2 \Big[t^2 u \Big(2 a_1 b_2 \big(x_1 x_2 (t_1 + t_2)(2t - u - s) - (x_1 b_2 t_1 + x_2 a_1 t_2)(u + s) \big) + \\
&+ \left[x_1 t_1 \left(2(a_1 b_2^2 + a_2 b_1^2) + 3 x_1 b_1 b_2 \right) + x_2 t_2 \left(2(a_1^2 b_2 + a_2^2 b_1) + 3 a_1 a_2 x_2 \right) \right] u + \\
&+ 4 x_1 x_2 t \left((a_1 b_2 + a_2 b_1) u + a_1 b_2 t \right) \Big) \Big] + \Big[a_1 \leftrightarrow a_2, b_1 \leftrightarrow b_2, t \leftrightarrow u \Big], \\
W_4 &= x_1^2 x_2^2 a_1 a_2 b_1 b_2 \Big[t \Big(a_1 a_2 b_1 b_2 u (t_1 + t_2)(t - u - s) + (a_1 b_2 + a_2 b_1)^2 t u^2 - \\
&- 2 a_1 b_2 t (s + u)(2 a_2 b_1 u - a_1 b_2 s) \Big) \Big] + \Big[a_1 \leftrightarrow a_2, b_1 \leftrightarrow b_2, t \leftrightarrow u \Big].
\end{aligned}
$$

The invariant variables: $s = (q_1 + q_2)^2$, $t = (q_1 - k_1)^2$, $u = (q_1 - k_2)^2$, $a_1 = 2k_1 \cdot P_2/S$, $a_2 = 2k_2 \cdot P_2/S$, $b_1 = 2k_1 \cdot P_1/S$, $b_2 = 2k_2 \cdot P_1/S$.

The amplitudes and squared matrix elements for the full set of $2 \to 2$ subprocesses with Reggeons in the initial state which give contribution to dijet production are presented in the work *M.A. Nefedov, V.A. Saleev, A. V Shipilova.* Dijet azimuthal decorrelations at the LHC in the parton Reggeization approach. Phys. Rev. D**87** (2013) 094030. The all squared matrix elements are checked to give the correct expressions in the Parton Model limit.

Dijet production: cross section.

Exploiting the hypothesis of high-energy factorization, we express the hadronic cross sections $d\sigma$ as convolutions of partonic cross sections $d\hat{\sigma}$ with unintegrated PDFs Φ_g^h of Reggeized gluons in the hadrons h.

$$\frac{d\sigma(pp \to ggX)}{dk_{1T}dy_1 dk_{2T}dy_2 d\Delta\varphi} = \frac{k_{1T}k_{2T}}{16\pi^3}\int dt_1 \int d\phi_1 \Phi_g^p(x_1, t_1, \mu^2)\Phi_g^p(x_2, t_2, \mu^2) \times \frac{\overline{|\mathcal{M}(RR \to gg)|^2}}{(x_1 x_2 S)^2},$$

where $k_{1,2T}$ and $y_{1,2}$ are final gluon transverse momenta and rapidities, respectively, and $\Delta\varphi$ is an azimuthal angle enclosed between the vectors $\vec{k}_{1T}$ and $\vec{k}_{2T}$,

$$x_1 = (k_1^0 + k_2^0 + k_1^z + k_2^z)/\sqrt{S}, \quad x_2 = (k_1^0 + k_2^0 - k_1^z - k_2^z)/\sqrt{S},$$

$$k_{1,2}^0 = k_{1,2T}\cosh(y_{1,2}), \quad k_{1,2}^z = k_{1,2T}\sinh(y_{1,2}).$$

Dijet production at the LHC: comparison with experiment.

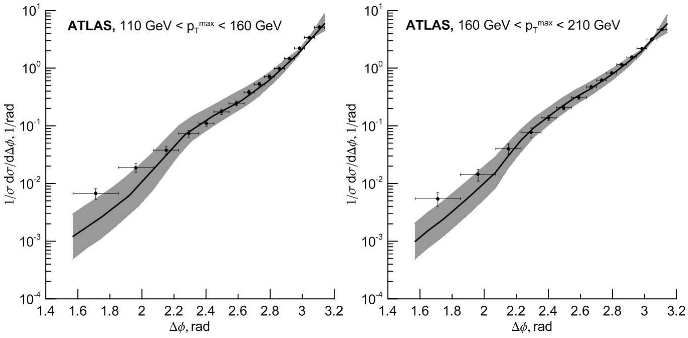

Figure 2 : The azimuthal dijet decorrelations at $\sqrt{S} = 7$ TeV, $|y_{jj}| < 1.1$

Dijet production at the LHC: comparison with experiment.

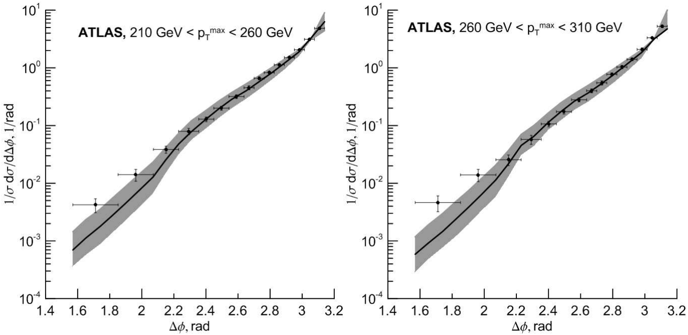

Figure 3 : The azimuthal dijet decorrelations at $\sqrt{S} = 7$ TeV, $|y_{jj}| < 1.1$

Dijet production at the LHC: comparison with experiment.

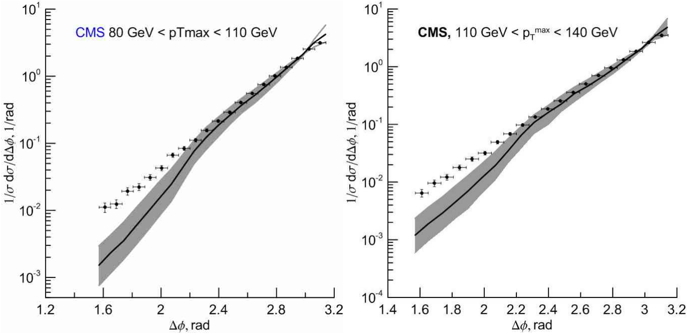

Figure 4 : The azimuthal dijet decorrelations at $\sqrt{S} = 7$ TeV, $|y_{jj}| < 1.1$

Dijet production at the LHC: comparison with experiment.

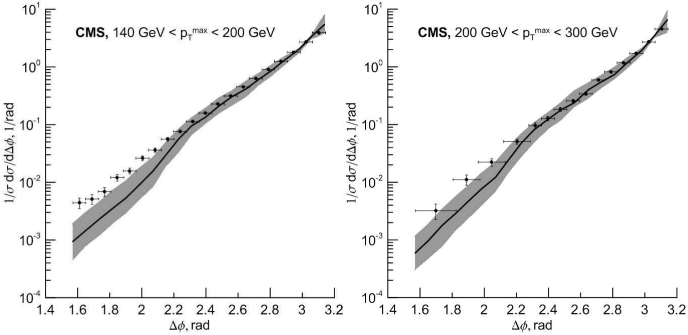

Figure 5 : The azimuthal dijet decorrelations at $\sqrt{S} = 7$ TeV, $|y_{jj}| < 1.1$

Dijet production at the LHC: comparison with experiment.

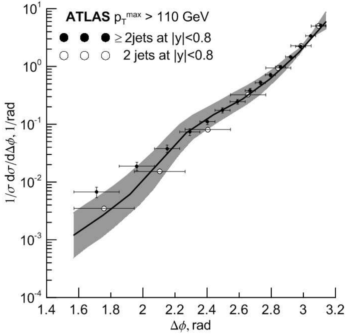

Figure 6 : The azimuthal dijet decorrelations at $\sqrt{S} = 7$ TeV, $|y_{jj}| < 1.1$

The next step of the analysis can be **an inclusion of a** $2 \to 3$ **process RR** $\to$ **ggg** to the calculations. That would lead to a more complete and precise description of the data which contain more than 2 jets in the final state.

Dijet production at the LHC: comparison with experiment.

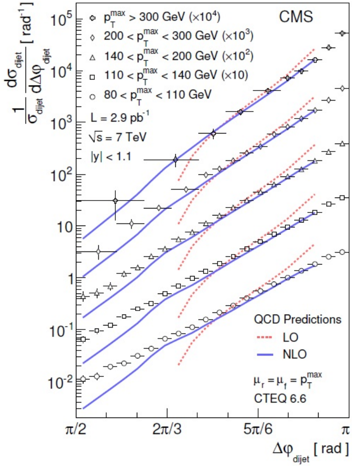

Figure 3: Normalized $\Delta\varphi_{\rm dijet}$ distributions in several $p_T{}^{\rm max}$ regions, scaled by the multiplicative factors given in the figure for easier presentation. The curves represent predictions from LO (dotted line) and NLO pQCD (solid line). Non-perturbative corrections have been applied to the predictions. The error bars on the data points include statistical and systematic uncertainties.

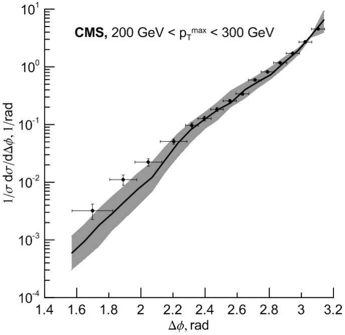

$b\bar{b}$-pair production at the LHC: comparison with experiment.

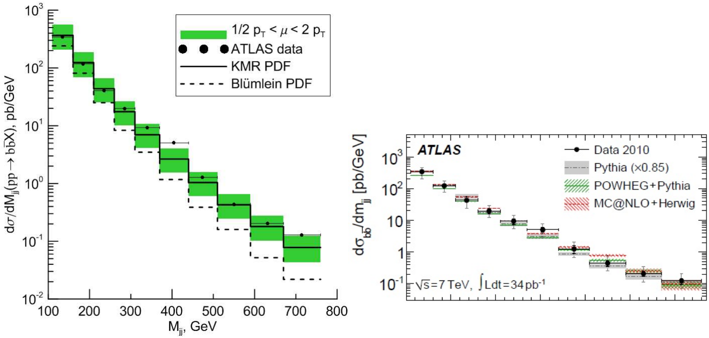

Figure 7 : The invariant mass spectra of $b\bar{b}$-pairs produced at $\sqrt{S} = 7$ TeV, $|y_{b,\bar{b}}| < 1.12$

$b\bar{b}$-pair production at the LHC: comparison with experiment.

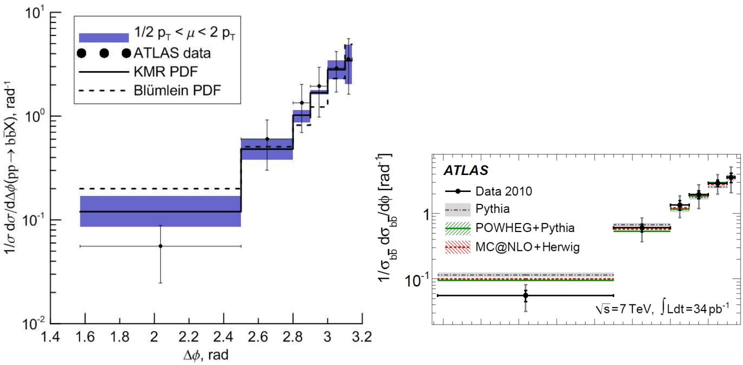

Figure 8 : The normalized azimuthal angle spectra of $b\bar{b}$-pairs produced at $\sqrt{S} = 7$ TeV, $|y_{b,\bar{b}}| < 1.12$

$b\bar{b}$-pair production at the LHC: comparison with experiment.

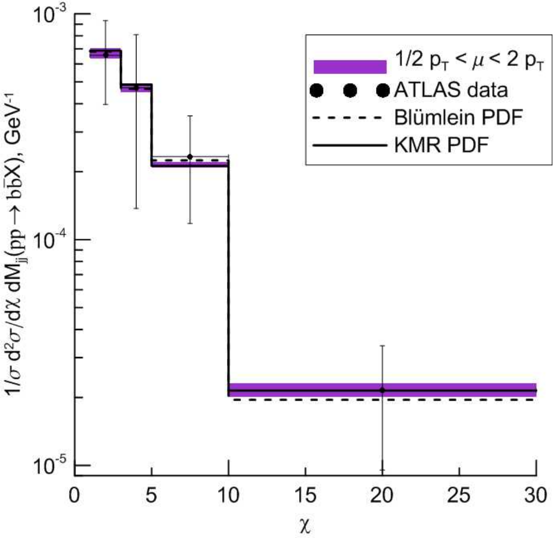

Figure 9 : The $b\bar{b}$-dijet cross-section as a function of χ for b-jets with $p_T > 40$ GeV, $|y| < 2.1$ and $|y_{boost}| = \frac{1}{2}|y_1 + y_2| < 1.1$, for dijet invariant mass range $110 < M_{jj} < 370$ GeV.

$b\bar{b}$-pair production at the LHC: comparison with experiment.

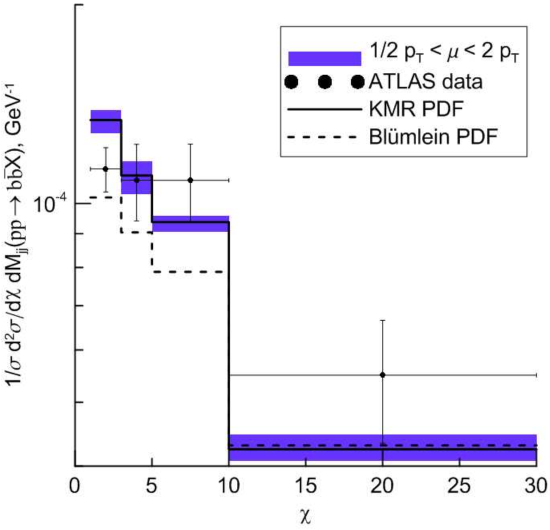

Figure 10 : The $b\bar{b}$-dijet cross-section as a function of χ for b-jets with $p_T > 40$ GeV, $|y| < 2.1$ and $|y_{boost}| = \frac{1}{2}|y_1 + y_2| < 1.1$, for dijet invariant mass range $370 < M_{jj} < 850$ GeV.

$b\bar{b}$-pair production at Tevatron: comparison with experiment.

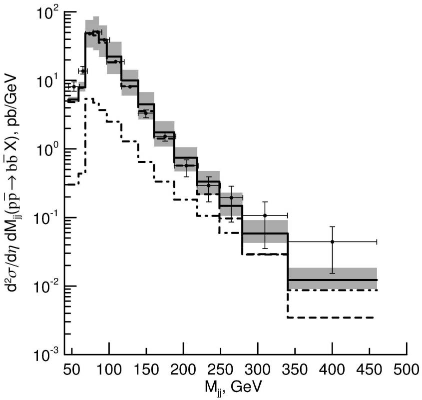

Figure 11 : The $b\bar{b}$-dijet cross-section as a function of the invariant mass of b-jets at $\sqrt{S} = 1.96$ TeV, $|\eta_{b,\bar{b}}| < 1.2$.

The contributions: $\mathcal{R} + \mathcal{R} \to b + \bar{b}$ (dash), $\mathcal{Q}_q + \bar{\mathcal{Q}}_q \to b + \bar{b}$ (dash-dot), sum of them both (solid).

$b\bar{b}$-pair production at Tevatron: comparison with experiment.

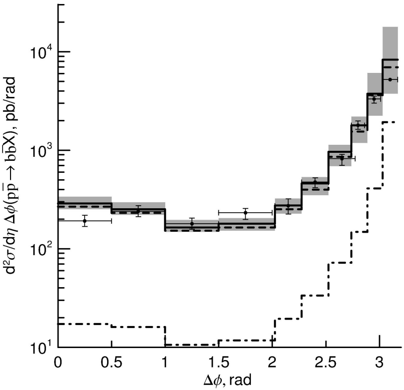

Figure 12 : The $b\bar{b}$-dijet cross-section as a function of the azimuthal angle between b-jets at $\sqrt{S} = 1.96$ TeV, $|\eta_{b,\bar{b}}| < 1.2$.

The contributions: $\mathcal{R} + \mathcal{R} \to b + \bar{b}$ (dash), $\mathcal{Q}_q + \bar{\mathcal{Q}}_q \to b + \bar{b}$ (dash-dot), sum of them both (solid).

$b\bar{b}$-pair production at Tevatron: comparison with experiment.

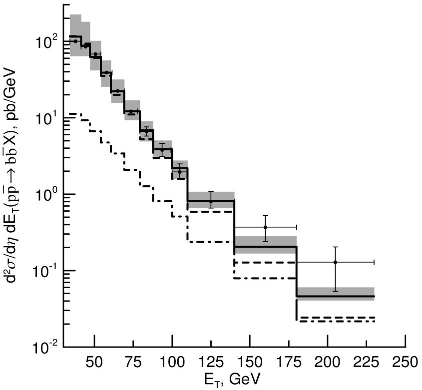

Figure 13 : The $b\bar{b}$-dijet cross-section as a function of the leading jet transverse energy for b-jets at $\sqrt{S} = 1.96$ TeV, $|\eta_{b,\bar{b}}| < 1.2$.

The contributions: $\mathcal{R} + \mathcal{R} \to b + \bar{b}$ (dash), $\mathcal{Q}_q + \bar{\mathcal{Q}}_q \to b + \bar{b}$ (dash-dot), sum of them both (solid).

Prompt-photon plus jet production at HERA: comparison with experiment.

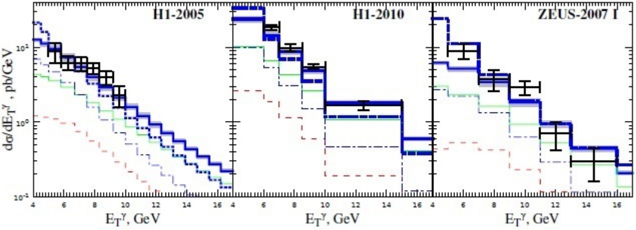

Figure 14 : E_T distributions of $pe \to \gamma + j + X$ under H1-2005 (left panel), H1-2010 (central panel), and ZEUS-2007 I (right panel) kinematic conditions. The experimental data are compared with LO PRA (boldfaced solid blue lines) and LO CPM (boldfaced dotted blue lines) predictions.

Prompt-photon plus jet production at HERA: comparison with experiment.

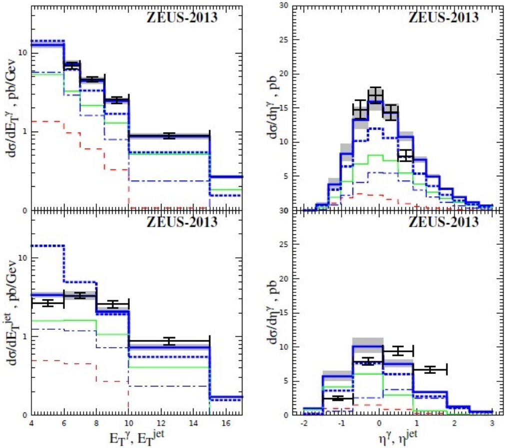

Figure 15 : E_T^γ (upper left panel), η^γ (upper right panel), E_T^{jet} (lower left panel), and η^{jet} (lower right panel) distributions of $pe \to \gamma + j + X$ under ZEUS-2013 kinematic conditions.

Summary

- The good description of dijet azimuthal decorrelations is achieved just in the LO parton Reggeization approach, without any ad-hoc adjustments of input parameters, whereas in the collinear parton model, such a degree of agreement calls for NLO and NNLO corrections and complementary initial-state radiation effects and ad-hoc nonperturbative transverse momenta of partons.
- *Prompt-photon plus jet associated photoproduction* *B. A. Kniehl, M. A. Nefedov, V. A. Saleev*. Prompt-photon plus jet associated photoproduction at HERA in the parton Reggeization approach. Accepted to Phys. Rev. D, arXiv: 1404.3513v2 [hep-ph].
- *Jet and Dijet production at the LHC*
  B. A. Kniehl, V. A. Saleev, A. V. Shipilova, E. V. Yatsenko. Single jet and prompt-photon inclusive production with multi-Regge kinematics: From Tevatron to LHC. Phys. Rev. D **84**, 074017 (2011);
  M. A. Nefedov, N. N. Nikolaev, V. A. Saleev. Drell-Yan lepton pair production at high energies in the parton Reggeization approach. Phys. Rev. D **87**, 014022 (2013).
  *M.A. Nefedov, V.A. Saleev, A. V Shipilova.*Dijet azimuthal decorrelations at the LHC in the parton Reggeization approach. Phys. Rev. D**87** (2013) 094030.
- *b−jet production at the LHC*
  B. A. Kniehl, A. V. Shipilova and V. A. Saleev. Inclusive b and b anti-b production with quasi-multi-Regge kinematics at the Tevatron. Phys. Rev. D **81**, 094010 (2010);
  V. A. Saleev and A. V. Shipilova. Inclusive b-jet and bb-dijet production at the LHC via Reggeized gluons. Phys. Rev. D **86**, 034032 (2012).
- *Heavy quarkonium production at the LHC*
  *M.A. Nefedov, V.A. Saleev, A. V. Shipilova.*Prompt Upsilon(nS) production at the LHC in the Regge limit of QCD. Phys. Rev. D**87** (2013)
  *M.A. Nefedov, V.A. Saleev, A. V. Shipilova.*Prompt J/psi production in the Regge limit of QCD: From Tevatron to LHC Phys. Rev. D**85** (2012) 074013.

Summary

- The good description of dijet azimuthal decorrelations is achieved just in the LO parton Reggeization approach, without any ad-hoc adjustments of input parameters, whereas in the collinear parton model, such a degree of agreement calls for NLO and NNLO corrections and complementary initial-state radiation effects and ad-hoc nonperturbative transverse momenta of partons.
- *Prompt-photon plus jet associated photoproduction* *B. A. Kniehl, M. A. Nefedov, V. A. Saleev*. Prompt-photon plus jet associated photoproduction at HERA in the parton Reggeization approach. Accepted to Phys. Rev. D, arXiv: 1404.3513v2 [hep-ph].
- *Jet and Dijet production at the LHC*
  B. A. Kniehl, V. A. Saleev, A. V. Shipilova, E. V. Yatsenko. Single jet and prompt-photon inclusive production with multi-Regge kinematics: From Tevatron to LHC. Phys. Rev. D **84**, 074017 (2011);
  M. A. Nefedov, N. N. Nikolaev, V. A. Saleev. Drell-Yan lepton pair production at high energies in the parton Reggeization approach. Phys. Rev. D **87**, 014022 (2013).
  *M.A. Nefedov, V.A. Saleev, A. V Shipilova.*Dijet azimuthal decorrelations at the LHC in the parton Reggeization approach. Phys. Rev. D**87** (2013) 094030.
- *b−jet production at the LHC*
  B. A. Kniehl, A. V. Shipilova and V. A. Saleev. Inclusive b and b anti-b production with quasi-multi-Regge kinematics at the Tevatron. Phys. Rev. D **81**, 094010 (2010);
  V. A. Saleev and A. V. Shipilova. Inclusive b-jet and bb-dijet production at the LHC via Reggeized gluons. Phys. Rev. D **86**, 034032 (2012).
- *Heavy quarkonium production at the LHC*
  *M.A. Nefedov, V.A. Saleev, A. V. Shipilova.*Prompt Upsilon(nS) production at the LHC in the Regge limit of QCD. Phys. Rev. D**87** (2013)
  *M.A. Nefedov, V.A. Saleev, A. V. Shipilova.*Prompt J/psi production in the Regge limit of QCD: From Tevatron to LHC Phys. Rev. D**85** (2012) 074013.

Summary

- The good description of dijet azimuthal decorrelations is achieved just in the LO parton Reggeization approach, without any ad-hoc adjustments of input parameters, whereas in the collinear parton model, such a degree of agreement calls for NLO and NNLO corrections and complementary initial-state radiation effects and ad-hoc nonperturbative transverse momenta of partons.
- *Prompt-photon plus jet associated photoproduction* *B. A. Kniehl, M. A. Nefedov, V. A. Saleev*. Prompt-photon plus jet associated photoproduction at HERA in the parton Reggeization approach. Accepted to Phys. Rev. D, arXiv: 1404.3513v2 [hep-ph].
- *Jet and Dijet production at the LHC*
  B. A. Kniehl, V. A. Saleev, A. V. Shipilova, E. V. Yatsenko. Single jet and prompt-photon inclusive production with multi-Regge kinematics: From Tevatron to LHC. Phys. Rev. D **84**, 074017 (2011);
  M. A. Nefedov, N. N. Nikolaev, V. A. Saleev. Drell-Yan lepton pair production at high energies in the parton Reggeization approach. Phys. Rev. D **87**, 014022 (2013).
  *M.A. Nefedov, V.A. Saleev, A. V Shipilova.*Dijet azimuthal decorrelations at the LHC in the parton Reggeization approach. Phys. Rev. D**87** (2013) 094030.
- *b−jet production at the LHC*
  B. A. Kniehl, A. V. Shipilova and V. A. Saleev. Inclusive b and b anti-b production with quasi-multi-Regge kinematics at the Tevatron. Phys. Rev. D **81**, 094010 (2010);
  V. A. Saleev and A. V. Shipilova. Inclusive b-jet and bb-dijet production at the LHC via Reggeized gluons. Phys. Rev. D **86**, 034032 (2012).
- *Heavy quarkonium production at the LHC*
  *M.A. Nefedov, V.A. Saleev, A. V. Shipilova.*Prompt Upsilon(nS) production at the LHC in the Regge limit of QCD. Phys. Rev. D**87** (2013)
  *M.A. Nefedov, V.A. Saleev, A. V. Shipilova.*Prompt J/psi production in the Regge limit of QCD: From Tevatron to LHC Phys. Rev. D**85** (2012) 074013.

Summary

- The good description of dijet azimuthal decorrelations is achieved just in the LO parton Reggeization approach, without any ad-hoc adjustments of input parameters, whereas in the collinear parton model, such a degree of agreement calls for NLO and NNLO corrections and complementary initial-state radiation effects and ad-hoc nonperturbative transverse momenta of partons.
- *Prompt-photon plus jet associated photoproduction* *B. A. Kniehl, M. A. Nefedov, V. A. Saleev*. Prompt-photon plus jet associated photoproduction at HERA in the parton Reggeization approach. Accepted to Phys. Rev. D, arXiv: 1404.3513v2 [hep-ph].
- *Jet and Dijet production at the LHC*
  B. A. Kniehl, V. A. Saleev, A. V. Shipilova, E. V. Yatsenko. Single jet and prompt-photon inclusive production with multi-Regge kinematics: From Tevatron to LHC. Phys. Rev. D **84**, 074017 (2011);
  M. A. Nefedov, N. N. Nikolaev, V. A. Saleev. Drell-Yan lepton pair production at high energies in the parton Reggeization approach. Phys. Rev. D **87**, 014022 (2013).
  *M.A. Nefedov, V.A. Saleev, A. V Shipilova.*Dijet azimuthal decorrelations at the LHC in the parton Reggeization approach. Phys. Rev. D**87** (2013) 094030.
- *$b-$jet production at the LHC*
  B. A. Kniehl, A. V. Shipilova and V. A. Saleev. Inclusive b and b anti-b production with quasi-multi-Regge kinematics at the Tevatron. Phys. Rev. D **81**, 094010 (2010);
  V. A. Saleev and A. V. Shipilova. Inclusive b-jet and bb-dijet production at the LHC via Reggeized gluons. Phys. Rev. D **86**, 034032 (2012).
- *Heavy quarkonium production at the LHC*
  *M.A. Nefedov, V.A. Saleev, A. V. Shipilova.*Prompt Upsilon(nS) production at the LHC in the Regge limit of QCD. Phys. Rev. D**87** (2013)
  *M.A. Nefedov, V.A. Saleev, A. V. Shipilova.*Prompt J/psi production in the Regge limit of QCD: From Tevatron to LHC Phys. Rev. D**85** (2012) 074013.

The advantages of the Parton Reggeization Approach

1. The gauge invariance of the initial off-shell quarks is held only in the Parton Reggeization Approach.

$$C_{QR,\ a}^{qg,\ b,\ \mu}(q_1,q_2,k_1,k_2)=\frac{1}{2}g_s^2\frac{q_2^-}{2\sqrt{t_2}}\bar{U}(k_1)\Big[\gamma_\sigma^{(-)}(q_1,k_1-q_1)t^{-1}\times$$
$$\times(\gamma_{\mu\nu\sigma}(k_2,-q_2)n_\nu^+ + t_2\frac{n_\mu^+ n_\sigma^+}{k_2^+})[T^a,T^b]-\gamma^+(\hat{q}_1-\hat{k}_2)^{-1}\gamma_\mu^{(-)}(q_1,-k_2)T^aT^b-$$
$$-\gamma_\mu(\hat{q}_1+\hat{q}_2)^{-1}\gamma_\sigma^{(-)}(q_1,q_2)n_\sigma^+T^bT^a+\frac{2\hat{q}_1 n_\mu^-}{k_1^-}\left(\frac{T^aT^b}{k_2^-}-\frac{T^bT^a}{q_2^-}\right)\Big],$$

2. The number of matrix elements obtained using the prescription of the k_t-factorization approach for off-shell gluon polarization vectors $\epsilon^\mu(q_T)=q_{T\mu}/\sqrt{\vec{q}_T^{\,2}}$ has the incorrect parton model limits $q_{1T},q_{2T}\to 0$, unlike the ones calculated in the Parton Reggeization Approach.

$$C_{RR}^{\mu,g}=\epsilon^\alpha(q_{1T})\epsilon^\beta(q_{2T})g_{\alpha\beta\mu}(q_1,q_2,q_1+q_2),\qquad C_{RR}^{q\bar{q}}=\epsilon^\alpha(q_{1T})\epsilon^\beta(q_{2T})M_{\alpha\beta}(gg\to q\bar{q})$$
$$C_{RR}^{gg,\mu\nu}\neq\epsilon^\alpha(q_{1T})\epsilon^\beta(q_{2T})M_{\alpha\beta}^{\mu\nu}(gg\to gg),\qquad C_{RQ}^{gq,\mu}\neq\epsilon^\alpha(q_{1T})M_\alpha^\mu(gq\to gq)$$

3. In the framework of Parton Reggeization Approach the NLO calculations can be correctly implemented.

The advantages of the Parton Reggeization Approach

1. The gauge invariance of the initial off-shell quarks is held only in the Parton Reggeization Approach.

$$C_{QR,\ a}^{qg,\ b,\ \mu}(q_1,q_2,k_1,k_2) = \frac{1}{2} g_s^2 \frac{q_2^-}{2\sqrt{t_2}} \bar{U}(k_1) \Big[\gamma_\sigma^{(-)}(q_1, k_1 - q_1) t^{-1} \times$$

$$\times (\gamma_{\mu\nu\sigma}(k_2, -q_2) n_\nu^+ + t_2 \frac{n_\mu^+ n_\sigma^+}{k_2^+}) [T^a, T^b] - \gamma^+ (\hat{q}_1 - \hat{k}_2)^{-1} \gamma_\mu^{(-)}(q_1, -k_2) T^a T^b -$$

$$-\gamma_\mu (\hat{q}_1 + \hat{q}_2)^{-1} \gamma_\sigma^{(-)}(q_1, q_2) n_\sigma^+ T^b T^a + \frac{2\hat{q}_1 n_\mu^-}{k_1^-} \left(\frac{T^a T^b}{k_2^-} - \frac{T^b T^a}{q_2^-} \right) \Big],$$

2. The number of matrix elements obtained using the prescription of the k_t-factorization approach for off-shell gluon polarization vectors $\epsilon^\mu(q_T) = q_{T\mu}/\sqrt{\vec{q}_T^2}$ has the incorrect parton model limits $q_{1T}, q_{2T} \to 0$, unlike the ones calculated in the Parton Reggeization Approach.

$$C_{RR}^{\mu,g} = \epsilon^\alpha(q_{1T})\epsilon^\beta(q_{2T}) g_{\alpha\beta\mu}(q_1, q_2, q_1 + q_2), \qquad C_{RR}^{q\bar{q}} = \epsilon^\alpha(q_{1T})\epsilon^\beta(q_{2T}) M_{\alpha\beta}(gg \to q\bar{q})$$

$$C_{RR}^{gg,\mu\nu} \neq \epsilon^\alpha(q_{1T})\epsilon^\beta(q_{2T}) M_{\alpha\beta}^{\mu\nu}(gg \to gg), \qquad C_{RQ}^{gq,\mu} \neq \epsilon^\alpha(q_{1T}) M_\alpha^\mu(gq \to gq)$$

3. In the framework of Parton Reggeization Approach the NLO calculations can be correctly implemented.

Thank you for attention!